Generic EIC-related Detector R&D Program

Imaging Calorimetry for the Electron-Ion Collider

Submission date: 25 July 2022

Whitney Armstrong, Sylvester Joosten, Jihee Kim, Manoj Jadhav, Jessica Metcalfe, Zein-Eddine Meziani, Chao Peng, Marshall Scott, Junqi Xie, Maria Żurek[1]

Argonne National Laboratory

Stjepan Orešić, Zisis Papandreou[2], Jonathan Zarling

University of Regina

Tony Affolder, Vitaliy Fadeyev

University of California, Santa Cruz

Wouter Deconinck

University of Manitoba

Abstract

Physics goals at the Electron-Ion Collider lead to unique requirements for electromagnetic calorimetry (ECAL) in the barrel region of the detector. The electron energy and shower profile measurements in the ECAL play a crucial role in the separation of electrons from background pions in Deep Inelastic Scattering processes. The calorimeter must also measure the energy and coordinates of photons, and identify single photons originating from, e.g. the Deeply Virtual Compton Scattering process, and photon pairs from the production of π^0s and their subsequent decay.

We propose an R&D program focused on the imaging calorimetry concept for the Electron-Ion Collider in the barrel region. The technology will allow for an accurate 3D imaging of particle showers by combining energy profiles, obtained with lead and scintillating fiber (Pb/ScFi) layers, with precise particle positions and single-hit energy information from several interleaved layers of monolithic silicon AstroPix sensors. This design provides considerably more information compared to traditional 2D calorimeters. The 3D nature of the images synergizes particularly well with event reconstruction approaches based on Machine Learning/Artificial Intelligence (ML/AI). This technology improves significantly the particle identification capabilities. For example, realistic simulation studies of AI/ML-based electron-pion separation show best-in-class performance at lower particle energies, while providing comparable results to state-of-the-art crystal calorimeters at higher energies at a significantly lower cost.

The generic R&D related to the hybrid imaging calorimetry for EIC calls for investigations of the Pb/ScFi and Astropix sensors technologies, as well as their integration. In this proposal, we plan to focus on questions targeting the ScFi technology, verifying with experimental data that it is capable of providing the required energy resolution in the barrel region of any EIC detector concept, as well as the position resolution crucial for position-matching of the clusters reconstructed from the imaging layers with the clusters from the Pb/ScFi section of the calorimeter. In FY23, we aim for a measurement at JLab Hall D, utilizing the existing Pb/ScFi GlueX prototype module, with electron energies higher than tested before in this type of calorimeter, to constrain the constant term of the energy resolution, which is important in the energy region of EIC. In addition to the SiPM readout, currently the most probable photosensor of choice for the sampling calorimtery at the EIC, we also aim for the very first precursory measurement with an MCP-PMT sensor providing excellent timing resolution and radiation hardness. In subsequent years we'll aim for measurements in the low energy range, as well as tests of the hadronic response in the Pb/ScFi.

[1]PI, Contact Person, zurek@anl.gov
[2]PI, Zisis.Papandreou@uregina.ca

Contents

1 Motivation

The Electron-Ion Collider (EIC) will address some of the most fundamental questions in nuclear physics, including the origin of the nucleon spin, the nucleon mass, the internal structure of nucleons and nuclei, and the properties of a dense system of gluons. Physics topics at the EIC lead to unique requirements for the electromagnetic calorimeter design, as described in [1]. Nearly all physics processes at the EIC require the detection of the scattered electron for momentum or energy reconstruction and particle identification. In the barrel region of the electromagnetic calorimeter (barrel ECAL) the momentum of electrons is measured with excellent precision ($\sigma_{p_T}/p_T(\%) = 0.1p_T \oplus 0.5$) with the tracker. However, the electron energy and shower profile measurements play a crucial role in separation of electrons from background pions in Deep Inelastic Scattering (DIS) processes. The ECAL must also measure energy and coordinates of neutral particles - mostly photons, and identify single photons originating from Deeply Virtual Compton Scattering (DVCS) process and photon pairs from π^0 decays.

The kinematic range of electrons from DIS, photons from DVCS, and π^0 particles from Semi-Inclusive DIS (SIDIS) simulated for e+p collisions at the highest beam energies of $18 \times 275\,\mathrm{GeV}/c$ is presented in Fig. 1.

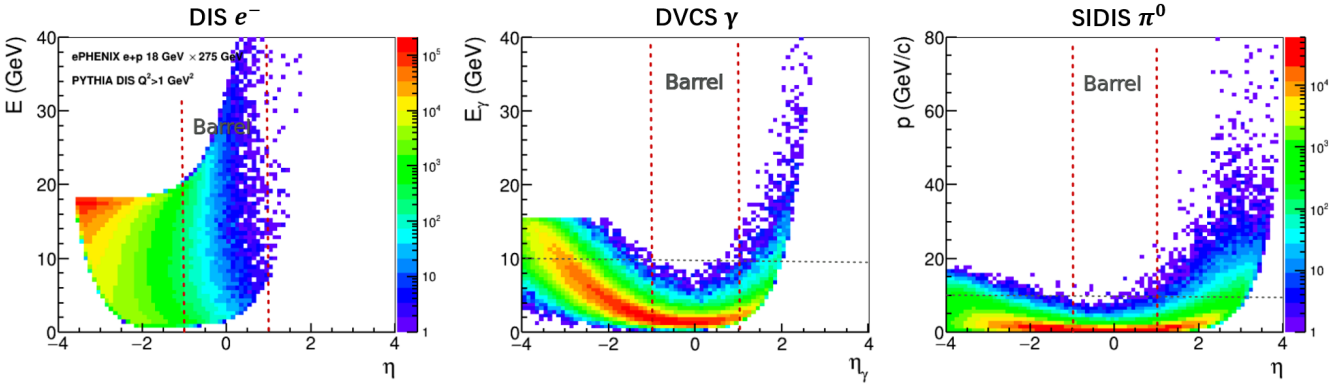

Figure 1: Momentum and energy of particles versus η from e+p collisions at beam energies of $18 \times 275\,\mathrm{GeV}/c$. The central barrel region of the electromagnetic calorimeter is marked with red dashed lines. The left plot presents the energy distribution of DIS electrons from PYTHIA simulations [2]. Electron energy varies from zero to the electron-beam energy in the backward region; and reaches higher energy up to about 40 GeV in the barrel region. The middle plot shows energy of photons from DVCS from the MILOU simulations [3]. The right plot shows π^0 momentum spectrum from SIDIS from PYTHIA simulations. In the barrel region the expected highest photon energy (π^0 momentum) is not higher than about 15 GeV (GeV/c). Plot adapted from [1].

1.1 Barrel ECAL Requirements

According to the EIC Yellow Report [1], the barrel region covering roughly $|\eta| < 1$, requires moderate energy resolution of approximately (10–12)%/$\sqrt{E} \oplus$ (1–3)%, however, with excellent electron-pion separation up to 10^4 in pion suppression at low particle-momenta below $4\,\mathrm{GeV}/c$; a good spatial resolution to separate photons from $\pi^0 \to \gamma\gamma$ decay with momentum up to about $15\,\mathrm{GeV}/c$; and the capability of detecting photons with energies down to $50 - 100\,\mathrm{MeV}$. As mentioned in the discussion of the Electromagnetic Calorimetry section of the EIC Yellow Report (Chapter 11, page 499), the required energy resolution mentioned above is sufficient for e/π separation at particle momenta above $4\,\mathrm{GeV}/c$ for studies of DIS processes in $e + p$ collisions at beam momenta of $18 \times 275\,\mathrm{GeV}/c$(the highest collision energy). The required separation for lower-momentum electrons and pions can only be achieved with particle identification coupled with calorimeters providing a much better resolution and/or by providing a shower-profile measurement capability, or by using different detectors, such as a Cherenkov detector. Moreover, the space for the ECAL calorimeter in the barrel region is limited (to about 40 cm) by the magnet design and may be further reduced by the additional space needed for a possible inner hadronic calorimeter.

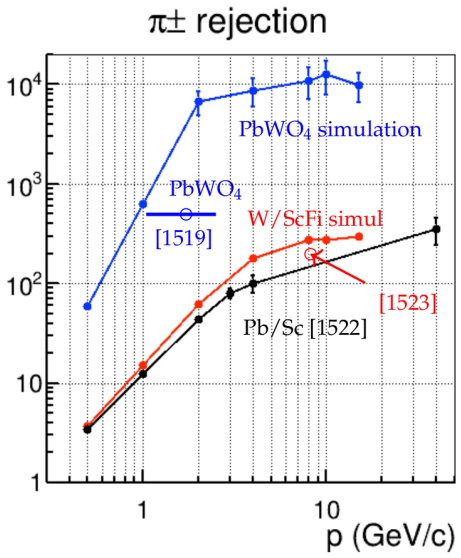

Figure 2: Measured and simulated pion rejection obtained with the E/p method with the $\Delta = 1.6\,\sigma_E/E$ cut (see text) for different detector technologies. The measured values for Pb/Sc shashlyk calorimeter (PHENIX, $8.1\%\sqrt{E} \oplus 2.1\%$) [5] are presented in black, simulations for W/ScFi calorimeter ($12\%\sqrt{E}\oplus 3\%$) and a measurement for 8 GeV [6] are presented in red, while the simulations for $PbWO_4$ ($2.5\%\sqrt{E} \oplus 1\%$), and a measurement at $1-2.5$ GeV [4] are presented in blue. Source: [1].

1.2 Performance with the Different Technologies Under Consideration

Figure 2 presents the measured and simulated pion rejection obtained with the E/p method for the detector technologies considered in the Yellow Report [1]. The method is based on the measured momentum of the charged track p and the energy deposited by this track in the calorimeter E, and requires $E/p > 1-\Delta$ to separate electrons from pions. All the curves in Fig. 2, including simulations and data, are obtained from the standalone calorimeter, *i.e.*, no other materials are placed in front of the calorimeter and no magnetic field is involved. Note that the rejection cut, $\Delta = 1.6\,\sigma_E/E$, uses the Gaussian width of the calorimeter signal, which for the Gaussian calorimeter response results in an electron efficiency of 95%. However, calorimeter responses typically have a lower energy tail, increased by material in front, which reduces the electron efficiency. The plot illustrates that the rejection based on E/p or one-dimensional shower profiles can only barely meet the pion suppression requirements for $PbWO_4$ at $p \geq 4\,\mathrm{GeV}/c$, and it is not sufficient for other technologies. Especially for the low momentum region at $p \leq 4\,\mathrm{GeV}/c$, one can see the drop in rejection power for all technologies, due to the intrinsic behavior of a calorimeter resulting in better performance with high-energy particles. It has been also pointed out in the Yellow Report that, while the results of calculations for sampling calorimeters are consistent with the measurements, the calculated pion suppression factor R_π is more than an order of magnitude higher than a measurement at 2.5 GeV [4]. It has been concluded that at this time we can not claim that a rejection power higher than 1000 is achievable at moderate energies even with the high-resolution $PbWO_4$ detector [1].

The ability to discriminate a single photon from the merged photon pair originating from π^0 decays depends on the π^0 momentum. The minimum angle between two photons in the lab frame from a high-momentum π^0 decay is $\sim (2m_{\pi^0})/p_{\pi^0}$, and most of the π^0 decays produce two photons at angles close to that minimal angle. The highest momentum at which the discrimination of a single photon from the merged photons from a π^0 decay is possible depends on the calorimeter granularity and spatial resolution. Usually, two photons are easily distinguishable in the ECAL when they are separated by a distance large enough to reconstruct two clusters. For modular calorimeters with large cells, one can separate photons down to the cell size. As shown in Fig. 1, in the barrel region, typical values for π^0 SIDIS momenta are up to $15\,\mathrm{GeV}/c$. Assuming required one-cell separation, one can discriminate π^0 and γ only up to about 7 GeV/c for 38 mm cell (close to the size considered for barrel ECAL cells) at calorimeter radius of 103 cm, and up to about 5 GeV/c at 80 cm radius (see Fig. 4).

1.3 Imaging Calorimetry for EIC Barrel Region

We propose an imaging calorimetry technology that is cost-effective in relation to its excellent performance in energy and spatial reconstruction and particle identification, fulfilling the Yellow Report requirements for the electromagnetic calorimeter in the barrel region and opening new opportunities with precise 3D shower imaging,

like, e.g., low energy muon identification or tagging final state radiative photons from nuclear/nucleon elastic scattering [7].

The concept for the silicon-sensor based imaging calorimeters, such as CALICE Si/W [8, 9] or CMS HGCAL [10], is based on thin silicon layers (of the order of about $100 - 500$ μm) as active material interleaved with thin (of the order of millimeters) layers of absorber (usually tungsten). Using high-granularity silicon sensors as active material allows for precise imaging of the 3D shower profile which enhances the particle identification capabilities or jet energy resolution through "particle flow" analysis relying on the reconstruction of as many particles in the jet as possible [8]. A challenging factor for this concept of calorimeters, that is important for the EIC, is the ratio of achievable energy resolution to the price of the calorimeter (number of silicon sensor layers which affects the sampling fraction).

For plastic-scintillator based sampling calorimeters, the contribution to the energy resolution by stochastic sampling fluctuations is described by:

$$\frac{\sigma_{\text{samp}}}{E} = \frac{a_{\text{samp}}}{\sqrt{E}}\,, \text{ where } a_{\text{samp}} \approx 2.7\%\sqrt{d/f_{\text{samp}}}\,. \tag{1}$$

In this formula, d is the thickness of the active sampling layer (in mm), and f_{samp} the sampling fraction for minimum ionizing particles. This approximate expression describes the energy resolution measured for a variety of different sampling calorimeters based on plastic scintillator well [11]. However, it does not hold for calorimeters with very thin (in terms of stopping power) active layers, such as silicon-based imaging calorimeters. For these calorimeters, pathlength fluctuations also contribute to the energy resolution. This is related to the fact that, for thin active layers, the energy deposited by typical for electromagnetic showers low-energy electrons, which are important for the shower development and energy resolution performance, depends on the pathlength in (i.e. the angle at which they traverse) an active layer. For example, for 500 μm silicon layers, this affects energy losses of electrons already above about 330 keV. For example, as pointed out in [11], the energy resolution for the CALICE Si/W prototype (525 μm layers) measured in the beam test is $\sim 16.5\%/\sqrt{E}$ [8], and the CMS HGCAL simulations give $\sim 19.9\%/\sqrt{E}$ (300 μm layers) and $\sim 24.3\%/\sqrt{E}$ (100 μm layers) [12], while the energy resolution formula from Eq. 1 gives $12\%/\sqrt{E}$ for all of these calorimeters, as they have about the same d/f_{samp}. Our early simulations, with 500 μm layers of silicon and tungsten showed similar resolutions of the order of $\sim$ (17–20)$\%/\sqrt{E}$ for about 20–22 layers of silicon sensors and different radial distribution of layers for $\sim 20X_0$. As the required energy resolution for the barrel region of EIC is (10–12)$\%/\sqrt{E} \oplus$ (1–3)% and we are searching for cost-effective solution, the pure Si/W imaging calorimeter is not a viable technology choice.

To leverage the imaging calorimetry particle identification capabilities, achieve required good energy resolution, and ensure a cost-effective solution with low risk, we propose a hybrid design utilizing scintillating fibers (ScFi) embedded in Pb, and imaging layers based on monolithic silicon sensors. In this concept, the imaging of particle showers is achieved by 6 layers of imaging Si sensors interleaved with 5 Pb/ScFi layers, followed by a large chunk of Pb/ScFi resulting in a total radiation thickness of about 20 X_0 contained in less than 40 cm of radial space.

The proposed technology for imaging layers can be based on the off-the-shelf AstroPix sensor [13], that is being designed using a 180 nm CMOS process for NASA's AMEGO-X mission [14]. AstroPix is the successor of ATLASPix [15], a low-power pixel detector developed for the ATLAS experiment, and further optimized for AMEGO-X. Tracking layers are a relatively new idea for calorimetry; however, it relies on the well-developed technology of CMOS pixel sensors. In particular, basing the design on the AstroPix detector provides an off-the-shelf technology (NASA is planning to have the AstroPix modules commercially manufactured). The first and second versions of the AstroPix detector are being tested [7], and a version 3a is already submitted and expected to be delivered in November 2022. This version would be a 2 cm $\times$ 2 cm quad chip, with 500 μm $\times$ 500 μm pixel size, 725 μm thickness and other parameters aimed at performance goals for AstroPix pixels based on [13]. The version 3a, along with modifications in chip and pixel geometry incorporates technical changes which deals with bug fixing observed during version 2 testings. The version 3a expected to have low power dissipation of less than 1 mW/cm^2 from pixel and digital contribution of 1 mW/APS. The chip will be integrated with temperature sensors with ADC and buffers. The chip will have improved SPI clock routing and shielding to reduce probability of cross talks between pixel rows and columns. The next, and most likely final, version 3b is planned to be submitted for production beginning of 2023. This family of sensors has demonstrated excellent energy resolution at low energies ($\sim$ 7% at 30 keV) and have very low power and cooling requirements (targeted power usage for AstroPix < 1mW/cm^2), as it is planned to be used in space. This technology was discussed in the EIC Yellow Report as an

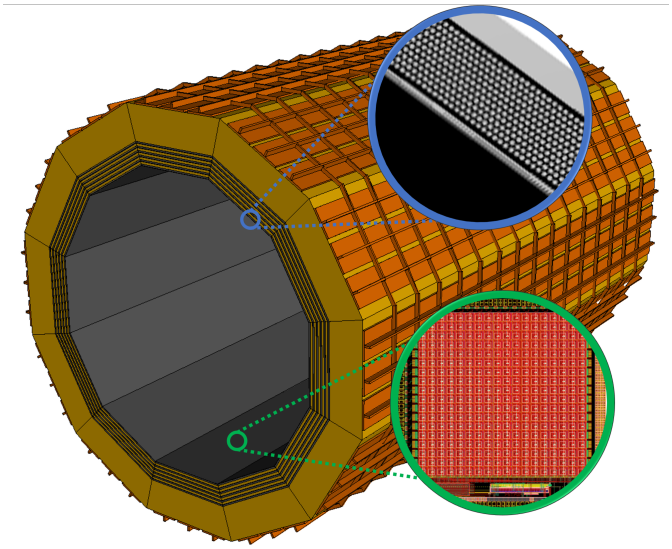

Figure 3: A possible imaging barrel calorimeter geometry as implemented in simulations. The innermost layer in every stave, which is the imaging AstroPix layer, is 405 cm long and about 55.2 cm wide. 6 layers of imaging Si sensors are interleaved with 5 Pb/ScFi layers, followed by a large chunk of Pb/ScFi. The thickness of the entire calorimeter (not including the support structure) is only about 40 cm.

alternative to light-collecting calorimeters.

The proposed Pb/ScFi layer design is based on the existing GlueX Barrel Calorimeter, presented in Fig. 6, with about 4 m-long scintillating fibers parallel to the beam with two side SiMP readout for spatial resolution along the z-coordinate (or pseudorapidity η). The GlueX Barrel Calorimeter quotes an energy resolution of $5.2\%/\sqrt{E}\oplus 3.6\%$ [16] (integrated over typical angular distributions for π^0 and η production) and z-position resolution $\sigma_z = 1.1\,\mathrm{cm}/\sqrt{E}$ at normal incident angle (Table 1 in [17]). The energy resolution has been obtained by fitting low-energy data ($< 2.5\,\mathrm{GeV}$) that do not fully constrain the constant term [16] (See the discussion about R&D needs in 2). The outer, thick layer of Pb/ScFi can contribute to hadronic final state reconstruction with an energy-flow algorithm, since, for example in the geometry described above, 70% or more of produced neutrons are expected to begin showering within the barrel ECAL [18, 19]. This information can be used to control for losses in the magnet material. Such an energy-flow approach, successfully applied by ALEPH, H1 and CMS among others, will improve the overall accuracy of hadronic reconstruction, jet-energy scale calibration, and missing-energy measurements. Moreover, the noise in barrel calorimeters was a key limitation for H1 DIS measurements at low y [20], as the performance of hadronic reconstruction methods is dominated by noisy clusters. The 3D information for clusters available will enable topological noise-suppression algorithms, which is a problem well suited for AI/ML applications as recent LHC studies suggest (see, e.g., Pileup Section in [21]).

This design is an alternative to the pointing geometry of the W/ScFi calorimeter considered for the barrel region in the Yellow Report. The Si imaging layers have an advantage in that they provide significantly better position resolution than can be achieved with any possible granularity for a W/ScFi calorimeter, and they provide a precise depth profile measurement of the shower, which is not measurable with the Yellow Report pointing W/ScFi. Pb/ScFi readout can be organized in radial layers and will provide additional information that can be used for shower profiling and improved energy resolution with respect to the Yellow Report requirements ($\sim 5\%/\sqrt{E}$). This design allows for significantly improved e/π separation and γ reconstruction.

Fig. 3 presents a possible geometry of the barrel electromagnetic calorimeter build with the hybrid imaging calorimety concept that has been included in the Geant4 simulations. In the picture the barrel is composed of 12 staves, however, this number is not fixed and will have to be adjusted in the future based on mechanical as well as readout properties. The inner radius of the barrel is 103 cm (presented geometry fits 3T solenoid geometry). Each stave is 405 cm long. The first (closest to the beam) layer in every stave is an imaging layer. Every imaging layer is separated by a Pb/ScFi layer with 13 rows of scintillating fibers that is about 1.59 cm thick. The width of each imaging layer increases with the radius. Every calorimeter stave has a total radial thickness of about 40 cm. In this geometry, the barrel ECAL contains the electromagnetic calorimeter endcap in the electron-going direction (i.e., it partially serves as the endcap electromagnetic calorimeter) covering the η range of about (-1.5, 1.1).

1.4 Simulated Performance of Proposed Hybrid Imaging Calorimeter

The design has been studied in detail through simulations and tested for the main requirements for the physics case of the Electron-Ion Collider described in the community Yellow Report for Detector I and II. In our simulations, we explored the possibility of using the AstroPix sensor off-the-shelf, with the performance parameters from [16]. In the Pb/ScFi simulations, we use the same plastic scintillator fiber size (radius $r = 0.5\,\text{mm}$) and distance between layers of fibers (radial pitch) equal to 1.22 mm and the azimuthal (lateral) pitch equal to 1.35 mm as in GlueX. The implemented readout follows the design of GlueX BCAL [22], but with larger granularity in the radial direction. The response of scintillating fibers is grouped in readout units of about 2×2 cm^2 (20 layers in radial direction and granularity in ϕ of about 1.1 deg).

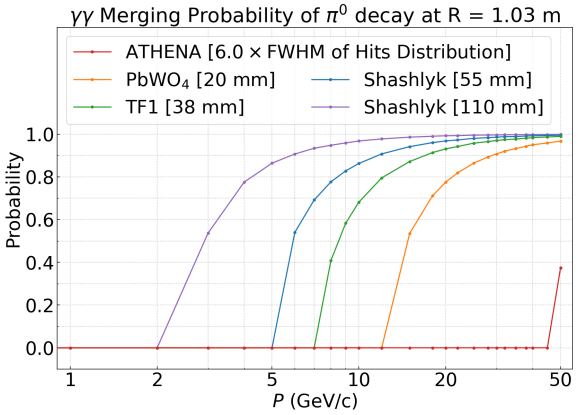

Figure 4: Simulated merging probability of the two γs from π^0 decay in the barrel region at $r = 103$ cm in the imaging barrel ECAL for the separation criteria of 6×FWHM of the shower profile (red). For the other technologies, one cell size is used to estimate the probability [1].

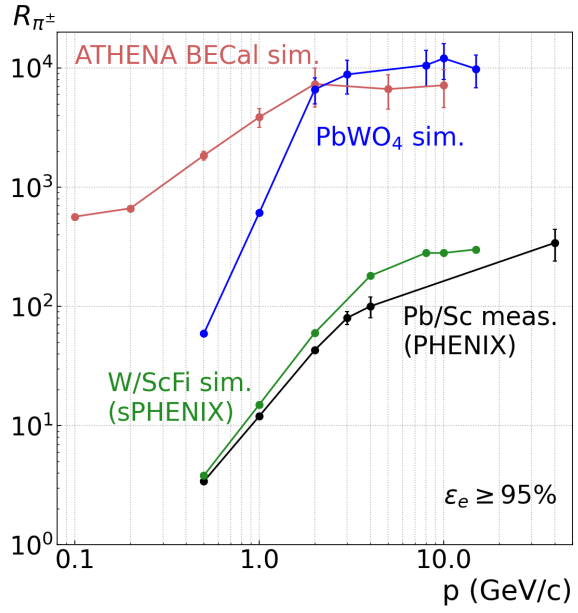

Figure 5: Simulated pion rejection power of the imaging barrel calorimeter (red solid line) in comparison to measured and simulated performance of other detector technologies [1], which are also presented on Fiq. 2 with additional data points. All the curves are obtained for the standalone calorimeter, *i.e.*, no other materials are placed in front of the calorimeter and no magnetic field is involved.

The results of these investigations, described in a technical note [7], show that the design fulfills and further improves the Yellow Report requirements for the electromagnetic barrel calorimeter in the central region. The simulated Pb/ScFi energy resolution is of the order of $\sigma/E = (5.3 \pm 0.1)\%/\sqrt{E} \oplus (0.73 \pm 0.05)\%$ for photons at normal incident angle. The imaging layers provide excellent spatial resolution and capability of 3D imaging of the shower, which allows, for example, to distinguish $\pi^0 \to \gamma\gamma$ decays from single photons at high energies (well above

20 GeV) and measure with high precision the coordinates of the photon's impact. The probability of merging two γs into one cluster at $r = 103\,\text{cm}$ is presented in Fig. 4. For different calorimeter technologies with large cells presented in the EIC Yellow Report [1] the minimal separation distance is taken as one cell size. For the imaging ECAL, the probability of merging two γs has been obtained using separation criteria of 6 $\times$ FWHM of the shower profile (taken at the third imaging layer for photons below 5 GeV/c and at the second layer for photons above 5 GeV/c; see [7] for more details).

Moreover, utilizing ML/AI techniques with the energy and position information from Pb/ScFi and imaging layers in addition to the E/p cut, the simulations show that the calorimeter will provide a pion-electron separation that is significantly better than that achievable with traditional sampling calorimetry, especially at lower particle energies. The performance is shown in Fig. 5 together with the pion rejection based on E/p method for other detector technologies taken from [1]. Simulations show that the AI-based electron-pion separation from 3D cluster profiles performs best-in-class at lower particle momenta ($p \leq 4\,\text{GeV}/c$), while providing comparable results to state-of-the-art crystal calorimeters at higher momenta at a significantly lower cost.

In summary, simulations show that this innovative, and cost-effective in relation to its performance, detector concept will provide excellent position resolution allowing precise 3D shower imaging on top of the excellent energy resolution provided by the Pb/ScFi calorimeter. The precise 3D imaging will take full advantage of the ML/AI techniques to unlock many benefits compared to traditional 2D calorimeters, for example:

- Significantly improved electron-pion separation with respect to the E/p method, especially in the low momentum region - impact on inclusive DIS cross section and asymmetries
- Separation of γs from π^0 decays at high momenta well above 20 GeV/c and precise position reconstruction of γs (well below 1 mm at 5 GeV/c) - impact on DVCS and photon physics
- Tagging final state radiative photons from nuclear/nucleon elastic scattering at low x to benchmark QED internal corrections, by precise measurement of photon coordinates and the angle between electrons and photons
- Allowing particle identification (PID) of low-energy muons that curl inside the barrel ECAL (below about 1.5 GeV/c with 3T magnetic field) - impact on J/ψ reconstruction and Timelike Compton Scattering (TCS)
- Improving particle identification based on other detector subsystems - providing space coordinate information for DIRC reconstruction (no need for additional large-radius tracking detector)

Additional assets of this technology are its compactness and the flexibility in varying the Pb to ScFi ratio, allowing to adjust or extend the outer thick layer of Pb/ScFi to serve as an inner hadronic calorimeter.

2 R&D Program

2.1 Goals

The generic R&D related to the hybrid concept of imaging calorimetry for EIC calls for investigations of the Pb/ScFi and Astropix sensors technologies, as well as the integration of both. In this proposal, we plan to focus on questions targeting the ScFi technology. In the upcoming FY23, we plan to start the R&D program utilizing one of the existing prototype modules constructed for the GlueX electromagnetic barrel calorimeter [16, 17]. We aim to use one of the GlueX Barrel ECAL prototype modules currently stored at the Thomas Jefferson National Accelerator (JLab) to measure its response to electromagnetic showers at energy ranges overlapping and beyond those tested in the GlueX experiment, especially at energies higher than those available in GlueX (see Sec. 2.2.2). The main goal of the planned beam test program is to obtain critical experimental data to cross-check the simulations of the electromagnetic (electrons/photons) response. These are essential for benchmarking the detector performance presented in the previous sections, as well as providing the input for future realistic studies (e.g. utilizing realistic recorded waveforms) on the Pb/ScFi part of the imaging calorimetry and on the integration with the AstroPix sensor layers. As a result of the planned beam tests, we aim for obtaining:

- **Energy resolution**, which affects, e.g., the pion-electron separation based on E/p method, and is needed for the four-momentum reconstruction, especially, of photons.

- **Timing resolution and related position resolution**, important for position-matching of the clusters reconstructed from imaging layers with the clusters from the Pb/ScFi calorimeter; this combined information is needed to reconstruct the full four-momentum of neutral particles.
- Estimated number of photoelectrons detected by photosensors as a function of particle energy to test the **linearity of the response**, important for energy measurements of wide energy range expected at the EIC, from about 100–200 MeV to above 40 GeV (for electrons) in the barrel region.

Moreover, the typical recorded waveforms during the beam test will serve as a simulation input for realistic studies of, e.g., the signal splitting of multiple particles hitting the same readout unit (multiplicity in ϕ). These simulations, in turn, will be further used to optimize the detector design, e.g., the granularity of the Pb/ScFi readout or location and number of imaging layers. We plan also to test, for the very first time, in addition to the SiPM readout, the readout with microchannel plate photomultipliers (MCP-PMTs) sensors to test possible achievable timing and position resolutions (see Sec. 2.2.4).

In the following FY24, as a continuation of this R&D program, we also plan to benchmark the responses to hadronic (charged pion) showers (see Sec. 2.2.3).

2.2 Details of Experimental Program

2.2.1 Prototype Module

We plan to use the the GlueX Barrel ECAL prototype module with the same structure of fibers and lead is as for the GlueX Barrel ECAL and as included in the imaging calorimeter simulation. The Kuraray SCSF-78MJ multi-clad scintillating fibers of 1 mm diameter are embedded between layers of lead of 0.5 mm thickness that were grooved creating channels to accommodate the fibers. The radial fiber pitch and the azimuthal fiber pitch are 1.22 mm and 1.35 mm, respectively. One smaller module (with ~ 58 cm long fibers) and one larger prototype (with ~ 1 m long fibers) are available at JLab, and can be used depending on available space in the test beam areas in experimental Halls. The modules are about 12 cm wide and 23 cm thick covering $\sim 15.5X_0$. One of them was machined along its long sides at an angle of 7.5 deg to match the trapezoidal geometry of the final GlueX barrel staves (see. Fig. 6). The modules can be read from both sides. The installation of the photosensors will be required in the preparation phase of the planned beam test.

2.2.2 Energy Consideration

The Pb/ScFi barrel electromagnetic calorimeters have been tested extensively in the lower energy range. The KLOE barrel ECAL has been exposed to photons with energies, on average, between 100 and 200 MeV and with very few photons greater than 400 MeV. For GlueX, about 30% of the photons registered in the barrel ECAL have energies considerably higher than 500 MeV, up to about 2.5 GeV. PYTHIA simulations, referred to in [23], indicate that $\sim 70\%$ of the produced photons with energies up to about 2 GeV are in the acceptance region of the GlueX barrel ECAL. The low-energy threshold for this calorimeter is $\sim (40-50)$ MeV which has been studied using Michel electrons, as described in [16]. Energies expected for the EIC at the highest beam energy setting (18×275 GeV/c) will be in the range of up to about 10 GeV for photons and up to 40 GeV for electrons (see Fig. 1). The lowest detectable energy according to the Yellow Report should be around 100 MeV [1].

The simulated energy resolution for a $\sim 20X_0$ imaging calorimeter is of the order of $\sigma/E = (5.3 \pm 0.1)\%/\sqrt{E} \oplus (0.73 \pm 0.05)\%$ for photons at normal incident angle. The value for the $\sim 15.5X_0$ GlueX barrel ECAL given in [16] is $5.2\%/\sqrt{E} \oplus 3.6\%$, which has a significantly larger constant term (even taking into consideration the difference in lengths of the calorimeters). This result is integrated over typical angular distributions for π^0 and η production for energy range of $0.5-2.5$ GeV. It has been noted that the response of the calorimeter averaged over its length for this energy range is not described well by the formula $\sigma/E = p_0/\sqrt{E} \oplus p_1$, and the fitted parameters are highly correlated (-0.89). Nevertheless, in order to characterize the performance of the GlueX barrel ECAL at $0.5-2.5$ GeV, the fitted parameters integrated over the angular distributions for π^0 and η were taken to characterize a typical energy resolution for the detector. To estimate the resolution at high energy, the authors used the simulations that described their data at low energy and, based on them, estimated a value for the constant term of less than 1.7% for a shallow impact angle of $12-13$ deg, and about 0.5% for an impact angle of $25-26$ deg (see Figures 32 and 33, and discussion on page 41 in [16]). While this result is similar to the one obtained in imaging ECAL simulations,

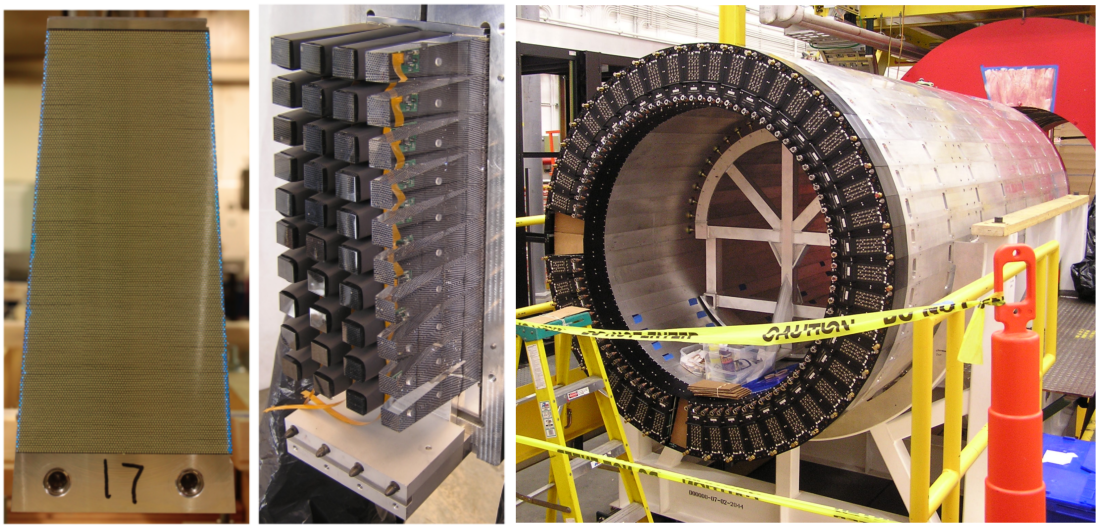

Figure 6: Left: Photo of the machined end of the Pb/ScFi matrix in one of the 48 GlueX barrel ECAL staves. Middle: Arrangement of light guides glued to the face of the matrix. Right: GlueX Barrel ECAL before insertion into the bore of the magnet. Source: [16]

one needs to verify this expectation with higher-energy data to fully constrain the constant term, which would be possible with the Hall D test measurement at up to 6.2 GeV/c in electron momenta. An experimental confirmation that the energy resolution in the simulations is realistic is important for the pion-electron separation based on E/p method and calorimeter performance for reconstructing photons. Measurements at low energies, closer to the lower limits of the design sensitivity at EIC, are important for the crucial input on the linearity of the detector responses and achievable energy resolution to validate the simulations.

2.2.3 Beam Particles Consideration

It is important to obtain the responses to both electromagnetic and hadronic showers in the Pb/ScFi part of the imaging calorimeter for the realistic input and cross-check of the detector performance. The reasoning for measurements of electron/photon showers at energies overlapping with and higher than those tested in the GlueX barrel ECAL have been detailed above. There is also a need for a crucial beam test with hadronic beams. As the Yellow Report [1] points out in the section related to the e/π discrimination, one should note that it is challenging to measure or calculate large rejection factors $R_\pi > 1000$ because of beam contamination or uncertainties in simulation of hadronic processes. Therefore, testing the energy response of the pions in Pb/ScFi is critical to make sure that the description of the hadronic showers in simulations is as realistic as possible. Experimental data with hadrons (pions, protons) will allow to benchmark the simulated responses including the description of quenching effects described by Birks' law [24]. The response to hadronic showers directly affects the e/π separation via E/p method. Moreover, since the Pb/ScFi calorimeter can also serve as an inner hadronic calorimeter, the responses to hadrons need to be well understood and included in realistic simulations.

2.2.4 Readout Consideration

As the barrel ECAL is located in a $> 1\,\mathrm{T}$ magnetic field, at the moment the natural cost-effective choice for the sensor technology is SiPM, which provides high gain (about 10^6) and a medium photodetection efficiency of about 20%. Therefore the priority for this FY is to perform the beam test with a matrix of SiPM readouts. As of now, we plan to use the available 40-SiPM prototype module assembly that fastens to one end of the prototype. The SiPMs are Hamamatsu S12045(X) Multi-Pixel Photon Counter (MPPC) arrays consisting of 16 tiles. Each tile is composed of 3600 $50 \times 50\,\mu\mathrm{m}^2$ pixels.

Some of the drawbacks of SiPMs are a limited dynamic range, intrinsic nonlinearity, noise, and susceptibility to radiation, in particular to neutron/proton radiation. The EIC Yellow Report lists moderate radiation hardness for the calorimetry, up to 3 kRad/year (30 Gy/year) electromagnetic and 10^{10} n/cm^2 hadronic at the top luminosity (for the barrel ECAL region, the numbers are of the order of 1 Rad/year and 10^8 n/cm^2) [1]. The SiPM radiation hardness has been tested by the GlueX collaboration that expects neutron fluence up to max $3-6\times10^8$ n/cm^2 in the barrel region [25, 26]. The results show that the dark rate seems to be significantly affected, which increases linearly with neutron dose at a rate of about 16 MHz per 10^9 n/cm^2. However, it has been estimated that running at a temperature of 5°C would extend the expected useful lifetime of the GlueX SiPMs at high intensity to about 7 years [27]. While more data on radiation hardness will be available from GlueX, STAR, and sPHENIX detectors, and the future developments of the SiPM are expected, other technologies may be also explored.

As a part of this R&D program we also plan to test, for the very first time, a calorimeter readout with MCP-PMT sensors. MCP-PMTs use microchannel plates to replace conventional discrete dynodes for electron signal amplification. They have been demonstrated [23, 28] to achieve excellent timing and position resolution, low noise, very high radiation tolerance, high granularity, and high magnetic field tolerance. However, the current generation of MCP-PMTs is very expensive, preventing their use for large-scale experiments due to cost concerns. The recently commercialized Large Area Picosecond Photo-Detector (LAPPD) provides a promising lower-cost photosensor alternative [29, 30]. Optimization of the photosensor design for high magnetic field tolerance, precision timing resolution, and pixelated readout was performed at ANL with 6×6 cm^2 MCP-PMTs [31], and a new 10×10 cm^2 MCP-PMT fabrication facility was manufactured and is currently under installation at ANL (commissioning planned in 2022). In case of possible delays with the commissioning of the ANL LAPPD facility, commercial 10×10 cm^2 MCP-PMT modules are planned be tested as in [32]. As this will be the very first attempt to read the Pb/ScFi calorimeter module with MCP-PMTs, our main goal is to obtain a reliable signal readout from the experimental setup. As this primary objective is accomplished, our investigation will focus on achievable energy, timing and, position resolutions. Similarly to the SiPM measurements, successfully recorded waveforms during the beam test will serve as a simulation input for realistic waveform analysis studies. This would allow us, for example, to study the possible lower limit of the energy and position separation from multiple showers hitting the same calorimeter readout unit, which expected to be improved by the timing/position resolution and narrower waveform of signals from MCP-PMT.

2.2.5 Beam Tests Schedule

To test the response of the Pb/ScFi calorimeter in both the low and high energy regions, we propose a set of comprehensive tests planned over the next years with electrons and pions:

1. For the benchmark at high energy (> 3 GeV) we aim for a beam test at JLab Hall D, located behind the Pair Spectrometer (PS) [33] allowing for measurement at electron momenta of about $3-6.2$ GeV/c (possibly down to 1.5 GeV/c with adjusted spectrometer configuration). This measurement is planned for the **FY23**. This measurement is strongly tied to the JLab Hall D schedule. It needs to happen before the long upgrade shutdown planned after March 2023, and requires only limited logistics. Therefore, it has the highest priority to be organized first.

2. To obtain the realistic input for simulations of charged pions in Pb/ScFi (in order to benchmark the Birks' law), we aim for a measurement of detector responses to hadronic showers utilizing an available pion beam at the Fermilab Beam Test Facility with momenta down to 1 GeV/c. This test is planned for **FY24**.

3. To test the responses to electromagnetic showers closer to the lower limits of the design sensitivity and in the region overlapping with typical energies at GlueX barrel ECAL, we aim to perform a measurement in JLab Hall B. In Hall B one can run a standalone test (without requiring signal from the Hall B trigger), positioning the prototype on the electron trajectory behind the photon tagger to select electrons of a given energy. The scheduling of this test is dependent of the schedule of Hall B experiments with low primary beam energies since the required Hall B tagger magnet can only operate with a beam energy below 6.1 GeV. We expect the most probable opportunity to be a parasitic run with the PRad-II experiment, which requested beam energies up to 3.3 GeV and will also use the tagger magnet for its detector calibration. The PRad-II experiment is working towards a schedule in **FY24-FY25**.

The Pb/ScFi module prototype is planned to be installed behind the Pair Spectrometer [33] in Hall D. In PS, electron-positron pairs are produced by beam photons interacting with a beryllium converter. The produced lepton pairs are deflected in a 1.5 T dipole magnet and detected using two layers of scintillation counters positioned symmetrically around the photon beam line. Each arm consists of 8 coarse counters and 145 high-granularity counters. The high-granularity hodoscope is used to measure the lepton momentum; the position of each counter corresponds to the specific energy. Each detector arm covers a range in lepton momentum of 3 GeV/c to 6.2 GeV/c. The energy resolution is estimated to be better than 0.6%. The position of the prototype will be aligned with respect to the beam line and PS position such a way that leptons enter the prototype perpendicular to the fibers direction. For signal digitization we plan to use 250 MHz flash ADCs [34] and F1 TDCs [35]. The prototype will be operated in standalone mode, parasitically to GlueX, using the PS trigger.

2.3 Research Program Schedule

Below is a table with the tasks, milestones, and deliverables for the R&D program in FY23 that summarizes the section above. This summary table is delineated by fiscal year quarter (Q).

Task	Goal date	Deliverable	Milestone
Objective I: Beam test at Hall D and data collection for electrons			
Preparation of online software for the beam test	Q1-Q2	Working module with readout and DAQ	
Preparation of the DAQ system	Q1-Q2	Working module with readout and DAQ	
Preparation of the module with attached SiPM readout	Q2	Working module with readout and DAQ	
Preparation of the module with MCP-PMT readout (after measurements with SiPMs)	Q2	Working module with readout and DAQ	
Installation of the module in Hall D PS area	Q2		ScFi prototype installed in Hall D ready to collect data
Beam test • Test of trigger and DAQ in the beam environment • Relative gain calibration of photosensors • Collection of TDC and ADC data (possibly with different electron energies and module incident angle, depending on opportunistic access to the area) with SiPM readout • Collection of TDC and ADC data with MCP-PMT	Q2	Collected experimental data • Data from beam test at high energy (above 3 GeV) electrons • Depending on the access to the experimental area data at lower energies, different impact angle ($\sim$ 45 deg) • First data with the MCP-PMT readout	Beam test accomplished and data collected
Objective II: Benchmarking and improving simulations			
Implementation of the prototype in Geant4 (within the dd4hep framework)	Q2	Characterization of energy and time response of Pb/ScFi part of imaging calorimeter for EM shower at higher energy	
Energy and time calibration of the data	Q2-Q3	Characterization of energy and time response of Pb/ScFi part of imaging calorimeter for EM shower at higher energy	
Extraction of energy, timing, position resolution and comparison with simulations	Q2-Q3	Characterization of energy and time response of Pb/ScFi part of imaging calorimeter for EM shower at higher energy	Data analyzed and simulation benchmarked
Implementation of the improved simulation responses in the full barrel ECAL simulation for further performance studies	Q4	Benchmarked simulations of EM shower response of Pb/ScFi part of imaging calorimeter for EM shower at higher energy	Improved, realistic simulations included in simulation framework

3 Budget

3.1 Nominal Budget

Funds requested for the FY23 are summarized in Tab. 1 which contains the baseline budget divided into cost subcategories and requesting institutions. More detailed breakdown of hardware and expense costs are presented in Tab. 2

	Argonne National Laboratory	University of Regina
Personnel	0	0
Hardware	$76K	0
Expenses including travel	$10K	$11K
Sum:	**$86K**	**$11K**

Table 1: Baseline budget for the Calorimetry R&D Project for FY23 with indication of the costs for personnel, hardware/property, and expenses including travel in USD.

Item	**Units**	**Price per unit (USD)**	**Total price (USD)**	**Source of price estimate**
VME crate	1	$16,500	$16,500	Old quote (2019)
Single board computer (SBC)	1	$8,000	$8,000	Old quote (2019)
PC	1	$2,000	$2,000	Current market prices (ANL provider website)
Rack-mountable server with fast hard drives	1	$7,000	$7,000	Current market prices (provider website)
FADC board (16 ch)	1	$6,500	$6,500	Old quote (2019)
TDC board (32 ch)	2	$5,500	$11,000	Old quote (2013) adjusted to 2022 USD
MPOD HV Module	1	$9,000	$9,000	Current Wiener quote
TI boards	1	$6,000	$6,000	Old quote (2019)
MCP-PMT readout PCB board	2	$5,000	$10,000	Expert opinion
Travel - ANL	5	$2,000	$10,000	Typical travel prices from ANL
Travel - Regina	2	$4,500	$9,000	Typical travel prices from Regina
Travel - Regina (from Pennsylvania)	1	$2,000	$2,000	Typical travel prices from Pennsylvania
TOTAL:			**$97,000**	

Table 2: Budget for the Calorimetry R&D Project for FY23 with breakdown of the estimated hardware and travel costs.

3.2 Budget Justification and Cost Effectiveness

To pursue the R&D program focused on questions related to the Pb/ScFi part of the imaging calorimetry, the support itemized in the budget Tab. 1 and Tab. 2 is requested. The budget contains two main parts, support for readout and DAQ hardware, and travel support.

The list of the hardware needs itemized in Tab. 2 includes equipment required to successfully establish the beam test program with Pb/ScFi and achieve the planned deliverables listed in Sec. 2.3 for FY23 and beyond. This includes readout of time and amplitude data from the SiPM modules to obtain the energy and timing resolution,

as well as the support for the MCP-PMT tests. The prices are based on current and old quotes and some expert opinion. The budget already takes into account readout and DAQ equipment that is already available for immediate and exclusive use from the resources of the Medium Energy Group at ANL for cost effectiveness. For example, 4 FADC units (with 16 channels each) are available, therefore only one such module is requested in the budget to read all 80 SiPM channels. As for the prototype module, we plan to reuse the existing prototype module with support equipment built for the GlueX barrel ECAL located at JLab, which reduces the amount of equipment needed to be purchased and/or shipped. FY23 cost is dominated by the one time cost of readout and DAQ hardware, that future beam tests listed in 2.2.5 will use.

The travel support has been estimated based on the typical travel cost for about 1-week-long visit at JLab when traveling from ANL or University of Regina. The travel funds for ANL will cover about 5 individual 1-week-long trips (3 staff scientists and 2 postdocs/students) or fewer but longer trips for the beam test. The travel support for University of Regina has been adjusted for the higher price of flights and longer stay for 2 people traveling from Canada, and one researcher traveling from Pennsylvania. To minimize the impact on cost and carbon footprint we will strive to optimize the travel logistics including time and duration of visits to the experimental facility and favouring domestic airlines for international travel. The travel funds estimate includes flight costs, per-diem, car rental, and accommodation at the JLab Residence Facility, and takes into account the travel time from Canada as well as additional time needed for Radiation Worker training and hall safety walk for new users.

3.3 Budget Scenarios

3.3.1 Nominal Budget Minus 20%

In the "nominal budget minus 20%" scenario our plan would be to resign from the purchases related to the MCP-PMT program (readout PCB boards and one-person travel costs **-$12K**) as well as reduce our hardware budget by about $8K. Depending on the availability of using Jefferson Lab equipment that is not currently in use by other projects we will, most probably, either resign from purchasing the server with hard drives (**-$7K**), or SBC (**-$8K**). The final decision will require further consultation with Hall D staff. The "minus 20%" scenario is summarized in Tab. 3.

	Argonne National Laboratory	University of Regina
Personnel	0	0
Hardware	$58K	0
Expenses including travels	$8K	$11K
Sum:	**$66K**	**$11K**

Table 3: The "minus 20%" scenario budget for the Calorimetry R&D Project for FY23 with indication of the costs for personnel, hardware/property, and expenses including travel in USD

In this scenario, the program related to MCP-PMTs will not happen during this FY year, and only measurement with the SiPM readouts will be performed. The deliverables and milestones will stay the same as described in the program schedule table in Sec. 2.3, but they will be obtained only for measurements with SiPMs.

3.3.2 Nominal Budget Minus 40%

In the "nominal budget minus 40%" we will further reduce the support for purchases related to the readout and DAQ. Depending on the availability of using Jefferson Lab equipment that is not currently in use by other projects, we will, most probably, either resign from purchasing the PC (**-$2K**) and VME Crate (**-$16.5K**) or the fADC and TDC boards (**-$17.5K**). The "minus 40%" scenario is summarized in Tab. 4.

In this scenario, we will resign from the MCP-PMT measurements, and depending on availability of VME crates and FADC and TDC boards that are not in use by other projects in Jefferson Lab in the 2nd quarter of FY23, we will need to adjust the measurements of the amplitude and timing signals from the 2-side readout of the prototype module. Not having all 40 readout units of both sides of the module available, will not allow us to test the full possible granularity of the signal readout up to $\sim 15.5X_0$ in depth, however we will still be able to obtain the overall energy resolution of the module and cross-check our simulations. Without the TDC modules, we won't be able

	Argonne National Laboratory	University of Regina
Personnel	0	0
Hardware	$39.5K	0
Expenses including travels	$8K	$11K
Sum:	**$47.5K**	**$11K**

Table 4: The "minus 40%" scenario budget for the Calorimetry R&D Project for FY23 with indication of the costs for personnel, hardware/property, and expenses including travel in USD.

to obtain the highest-resolution timing measurement and characterize the full potential for the position resolution of the module. We believe, however, that it is the worst case scenario, and we will be able to borrow the TDC modules to meet the goals of or program (possibly will need to use the travel funds for that). The schedule and milestones will stay the same as described in the program schedule table in Sec. 2.3, but they will be obtained only for measurements with SiPMs, and in the worst case scenario, we won't be able to deliver the measurement for the timing and position resolution with the expected in the real experiment resolution.

3.4 Money Matrix

	Beam test in Hall D w/ SiPMs	Beam test in Hall D w/ MCP-PMTs	Sum
Argonne National Laboratory	$74K	$12K	$86K
University of Regina	$11K	0	$11K
Sum	$85K	$12K	$97K

Table 5: Money matrix for the baseline budget itemizing the budget allocations to the individual institutions and the area of research. Note that the hardware equipment included in the SiPM part of the program is also needed for the measurements with MCP-PMTs (it is common for both programs). The cost under the MCP-PMT part of the program includes hardware needed to be purchased exclusively for the MCP-PMT measurement on top of that and one-person travel cost to JLab from ANL.

4 Diversity, Equity, and Inclusion

To be able to address the complex challenges that researchers belonging to historically underrepresented groups in science are forced to face in their career, it is imperative that all members of the scientific community join forces to ensure that current and future generations have access to a more inclusive, equitable, and diverse research environment. Our plan within the scope of this R&D program is to follow an "act locally, think globally" approach, by focusing our efforts on aspects that are directly within our control, and continue to participate to the wider mission to advance diversity, equity, and inclusion within our home institutions, the DOE, and the scientific community worldwide.

Mentorship and Student Recruiting Both formal studies and our own experience have shown the importance of researchers in positions of leadership actively embracing their role as mentors and advocates for students and researchers at earlier stages of their career. Programs that facilitate research internships at the undergraduate level and below represent a unique opportunity, as they have the potential to provide a wide range of benefits:

- For the participating students: financial support, the ability to gain valuable skills and work experience within a cutting-edge R&D program with applications to both industry and basic research
- For the project team: broadening the talent pool, establishing connections with teaching institutions, and ultimately taking concrete steps toward ensuring a greater diversity of backgrounds in the team's members

- For the scientific community, by actively contributing to the efforts aimed at undoing the effects of longstanding systemic issues such as lacking or unequal access to work opportunities, biased hiring practices, "leaky pipeline" phenomenon

At the level of our R&D program, we commit to actively seek and support the participation of students in our research activities. To maximize the positive impact of our actions and ensuring more equitable access for a broader, more diverse pool of candidates, we will consciously adopt practices aimed at addressing and reducing bias into the recruiting and selection process. The MEP group at ANL has already accrued considerable experience with participating in research programs for undergraduate students, such as DoE SULI or Minority Traineeship Programs. Throughout the years, we have been able to support students coming from a broad range of academic institutions, work experience, and backgrounds, and successfully supported them towards the completion of their internships at ANL. To further improve on this, we will be actively investigating other avenues to expand our reach for perspective applicants, for example by engaging with more local schools, universities, and community colleges in the vicinity of ANL.

Community Outreach and Science Education Being able to communicate the importance of our research to the general public, as well as transmitting our scientific passion to the next generation of scientists, is a continuing challenge for any publicly-funded research endeavor. Thanks to our expertise, we are confident in our ability to efficiently prepare for participation in various outreach and community engagement initiatives available through ANL or virtually. For example, a (suitably simplified) version of our experimental setup showcasing the basics of particle detection and the physics goals of the EIC can be presented as an engaging hands-on exhibit at science fairs, laboratory open days, for example at the ANL Open House (initiative led by Żurek and Kim) or APS Conference for Undergraduate Women in Physics (Żurek and Reimer are members of the Local Organizing Committee). In addition, we will work on ensuring that both our R&D activities and the wider scientific mission of the EIC can reach general audiences by leveraging our wide network of science communication avenues such as webpages, panels, podcasts, etc. (see, e.g., [36]). Members of our consortium have extensive experience in these regards. For instance, Żurek participated in a wide variety of volunteer initiatives for scientific outreach for audiences of all ages and backgrounds, including programs targeted more specifically to under-resourced schools and communities. In 2020, she became the first recipient of the Berkeley Lab K-12 Program Teaching Scholar certification [37], recognizing her commitment to science education and outreach through more than 200 volunteer-hours contributed to the program.

Establishing a safe and welcoming work environment for all This is critical for the success of any team activity across its lifetime: talent acquisition, retention, and overall performance and satisfaction. Building on the team's experience, we will actively implement practices to uphold principles such as psychological safety, inclusivity, and accountability. For instance, Żurek was one of the original proponents and stewards of the initiative leading to the creation of a formal Code of Conduct (CoC) for the Berkeley Lab Postdoc Association and related events (workshops, conferences, Slack workspaces etc.). Moreover, Deconinck was one of the members of the DEI committee of the EIC Users Group actively working on the CoC. When appropriately enforced, a CoC is a valuable tool to improve transparency and accountability, ensuring that the intended guidelines for inclusive behavior within the community are actually observed by all, ultimately resulting in greater psychological safety and participation in the community. This is particularly relevant for members of underrepresented groups, who could otherwise feel powerless to speak up in circumstances where the community guidelines are ignored or violated. We will incorporate a CoC for our online and in-person meetings as well as communication platform.

References

[1] R. Abdul Khalek *et al.*, "Science Requirements and Detector Concepts for the Electron-Ion Collider: EIC Yellow Report," 3 2021.

[2] T. Sjostrand, S. Mrenna, and P. Z. Skands, "A Brief Introduction to PYTHIA 8.1," *Comput. Phys. Commun.*, vol. 178, pp. 852–867, 2008.

[3] E. Perez, L. Schoeffel, and L. Favart, "MILOU: A Monte-Carlo for deeply virtual Compton scattering," 11 2004.

[4] S. Inaba, M. Kobayashi, M. Nakagawa, T. Nakagawa, H. Shimizu, K. Takamatsu, T. Tsuru, and Y. Yasu, "A Beam test of a calorimeter prototype of PWO crystals at energies between 0.5-GeV and 2.5-GeV," *Nucl. Instrum. Meth. A*, vol. 359, pp. 485–491, 1995.

[5] T. C. Awes *et al.*, "High-energy beam test of the PHENIX lead scintillator EM calorimeter," 2 2002.

[6] C. A. Aidala *et al.*, "Design and Beam Test Results for the sPHENIX Electromagnetic and Hadronic Calorimeter Prototypes," *IEEE Trans. Nucl. Sci.*, vol. 65, no. 12, pp. 2901–2919, 2018.

[7] ATHENA Proto-Collaboration, "Barrel Electromagnetic Calorimeter for the Electron-Ion Collider, supplemental material to the detector proposal." https://anl.app.box.com/s/w5i3e7cmzgznnl1qyjukuhspsn87zwhe, https://wiki.bnl.gov/athena/index.php/Supplemental_Material, 2021.

[8] F. Sefkow, A. White, K. Kawagoe, R. Pöschl, and J. Repond, "Experimental tests of particle flow calorimetry," *Rev. Mod. Phys.*, vol. 88, p. 015003, Feb 2016.

[9] D. Breton, A. Irles, J. Jeglot, J. Maalmi, R. Pöschl, and D. Zerwas, "CALICE SiW ECAL - Development and performance of a highly compact digital readout system," *JINST*, vol. 15, no. 05, p. C05074, 2020.

[10] B. Acar *et al.*, "Response of a CMS HGCAL silicon-pad electromagnetic calorimeter prototype to 20–300 GeV positrons," *JINST*, vol. 17, no. 05, p. P05022, 2022.

[11] R. Wigmans, "New developments in calorimetric particle detection," *Prog. Part. Nucl. Phys.*, vol. 103, pp. 109–161, 2018.

[12] D. Contardo, M. Klute, J. Mans, L. Silvestris, and J. Butler, "Technical Proposal for the Phase-II Upgrade of the CMS Detector," tech. rep., Geneva, Jun 2015. Upgrade Project Leader Deputies: Lucia Silvestris (INFN-Bari), Jeremy Mans (University of Minnesota) Additional contacts: Lucia.Silvestris@cern.ch, Jeremy.Mans@cern.ch.

[13] I. Brewer, M. Negro, N. Striebig, C. Kierans, R. Caputo, R. Leys, I. Peric, H. Fleischhack, J. Metcalfe, and J. Perkins, "Developing the future of gamma-ray astrophysics with monolithic silicon pixels," *Nuclear Instruments and Methods in Physics Research Section A: Accelerators, Spectrometers, Detectors and Associated Equipment*, vol. 1019, p. 165795, 2021.

[14] H. Fleischhack, "AMEGO-X: MeV gamma-ray Astronomy in the Multi-messenger Era," *PoS*, vol. ICRC2021, p. 649, 2021.

[15] A. Schöning *et al.*, "MuPix and ATLASPix – Architectures and Results," *PoS*, vol. Vertex2019, p. 024, 2020.

[16] T. D. Beattie *et al.*, "Construction and Performance of the Barrel Electromagnetic Calorimeter for the GlueX Experiment," *Nucl. Instrum. Meth. A*, vol. 896, pp. 24–42, 2018.

[17] B. D. Leverington *et al.*, "Performance of the prototype module of the GlueX electromagnetic barrel calorimeter," *Nucl. Instrum. Meth. A*, vol. 596, pp. 327–337, 2008.

[18] M. Anelli, S. Bertolucci, C. Bini, P. Branchini, G. Corradi, C. Curceanu, G. De Zorzi, A. Di Domenico, B. Di Micco, A. Ferrari, and et al., "Measurement of neutron detection efficiency between 22 and 174mev using two different kinds of pb-scintillating fiber sampling calorimeters," *Nuclear Instruments and Methods in Physics Research Section A: Accelerators, Spectrometers, Detectors and Associated Equipment*, vol. 617, p. 107–108, May 2010.

[19] M. Anelli, S. Bertolucci, C. Bini, P. Branchini, G. Corradi, C. Curceanu, G. De Zorzi, A. Di Domenico, B. Di Micco, A. Ferrari, and et al., "Measurement of the neutron detection efficiency of a 80% absorber–20% scintillating fibers calorimeter," *Nuclear Instruments and Methods in Physics Research Section A: Accelerators, Spectrometers, Detectors and Associated Equipment*, vol. 626-627, p. 67–71, Jan 2011.

[20] M. Peez, B. Portheault, and E. Sauvan, "An energy flow algorithm for Hadronic Reconstruction in OO: Hadroo2." https://marh1.in2p3.fr/doc/h1-0105-616.pdf.

[21] "A Living Review of Machine Learning for Particle Physics, Pileup." https://iml-wg.github.io/HEPML-LivingReview/.

[22] E. S. Smith, "Development of silicon photomultipliers and their applications to gluex calorimetry," *AIP Conference Proceedings*, vol. 1753, no. 1, p. 070006, 2016.

[23] Y. Ilieva, L. Allison, T. Cao, G. Kalicy, P. Nadel-Turonski, K. Park, C. Schwarz, J. Schwiening, and C. Zorn, "MCP-PMT studies at the High-B test facility at Jefferson Lab," *JINST*, vol. 11, no. 03, p. C03061, 2016.

[24] J. B. Birks, "Scintillations from organic crystals: Specific fluorescence and relative response to different radiations," *Proceedings of the Physical Society. Section A*, vol. 64, pp. 874–877, oct 1951.

[25] Y. Qiang, C. Zorn, F. Barbosa, and E. Smith, "Radiation Hardness Tests of SiPMs for the JLab Hall D Barrel Calorimeter," *Nucl. Instrum. Meth. A*, vol. 698, pp. 234–241, 2013.

[26] Y. Qiang, C. Zorn, F. Barbosa, and E. Smith, "Neutron radiation hardness tests of SiPMs," *AIP Conf. Proc.*, vol. 1560, no. 1, pp. 703–705, 2013.

[27] G. Collaboration, "Hall d / gluex technical construction report." https://halldweb.jlab.org/doc-public/DocDB/ShowDocument?docid=2511&version=5, Technical report, Jefferson Lab, April 2016.

[28] A. Lehmann *et al.*, "Recent progress with microchannel-plate PMTs," *Nucl. Instrum. Meth. A*, vol. 952, p. 161821, 2020.

[29] M. Minot, B. Adams, M. Aviles, J. Bond, T. Cremer, M. Foley, A. Lyashenko, M. Popecki, M. Stochaj, W. Worstell, M. Wetstein, J. Elam, A. Mane, O. Siegmund, C. Ertley, H. Frisch, A. Elagin, E. Angelico, and E. Spieglan, "Large area picosecond photodetector (lappdtm) - pilot production and development status," *Nuclear Instruments and Methods in Physics Research Section A: Accelerators, Spectrometers, Detectors and Associated Equipment*, vol. 936, pp. 527–531, 2019. Frontier Detectors for Frontier Physics: 14th Pisa Meeting on Advanced Detectors.

[30] M. J. Minot, D. C. Bennis, J. L. Bond, C. A. Craven, A. O'Mahony, J. M. Renaud, M. E. Stochaj, J. W. Elam, A. U. Mane, M. W. Demarteau, R. G. Wagner, J. B. McPhate, O. Helmut Siegmund, A. Elagin, H. J. Frisch, R. Northrop, and M. J. Wetstein, "Pilot production & commercialization of lappd™," *Nuclear Instruments and Methods in Physics Research Section A: Accelerators, Spectrometers, Detectors and Associated Equipment*, vol. 787, pp. 78–84, 2015. New Developments in Photodetection NDIP14.

[31] J. Xie, M. Chiu, E. May, Z. E. Meziani, S. Nelson, and R. Wagner, "MCP-PMT development at Argonne for particle identification," *JINST*, vol. 15, no. 04, p. C04038, 2020.

[32] C. Peng *et al.*, "Performance of photosensors in a high-rate environment for gas Cherenkov detectors," 11 2020.

[33] F. Barbosa, C. Hutton, A. Sitnikov, A. Somov, S. Somov, and I. Tolstukhin, "Pair spectrometer hodoscope for Hall D at Jefferson Lab," *Nucl. Instrum. Meth. A*, vol. 795, pp. 376–380, 2015.

[34] F. e. a. Barbosa, "A vme64x, 16-channel, pipelined 250 msps flash adc with switched serial (vxs) extension." https://halldweb.jlab.org/doc-public/DocDB/ShowDocument?docid=1022, Technical report, Jefferson Lab, April 2008.

[35] F. e. a. Barbosa, "The jefferson lab high resolution time-to-digital converter (tdc)." https://halldweb.jlab.org/doc-public/DocDB/ShowDocument?docid=1021, Technical report, Jefferson Lab, April 2008.

[36] M. Zurek and M. Diefenthaler, "Strong interactions podcast." https://www.stronginteractions.org/, 2022.

[37] Lawrence Berkeley National Laboratory, K-12 Office, "Berkeley Lab Teaching Scholars." https://k12education.lbl.gov/volunteer/teaching-scholars, 2020.